Modified axial pullout resistance factors of geostrip and metal strip reinforcements in sand considering transverse pull effects

Bhargav Kumar Karnamprabhakara
Indian Institute of Technology Hyderabad
Hariprasad Chennarapu
Mahindra École Centrale: Mahindra Ecole Centrale
Umashankar Balunaini (buma@ce.iith.ac.in)
Indian Institute of Technology Hyderabad

Research Article

Keywords: Reinforced soil, Geostrap, Metal strip, Axial pullout, Transverse pullout

Posted Date: March 2nd, 2023

DOI: https://doi.org/10.21203/rs.3.rs-2630871/v1

Additional Declarations:
Table 1 is available in the Supplementary Files section.

Modified axial pullout resistance factors of geostrip and metal strip reinforcements in sand considering transverse pull effects

Bhargav Kumar Karnamprabhakara[a], Hariprasad Chennarapu[b], Umashankar Balunaini[c]

[a]Post-Doctoral Fellow, Department of Civil Engineering, IIT Hyderabad, Kandi, Telangana 502284, India, Email: karnambhargav@gmail.com

[b]Associate Professor, Ecole Centrale School of Engineering, Mahindra University, Hyderabad, Telangana 500043, India. Email: hari.chennarapu@mahindrauniversity.edu.in

[c]Corresponding Author, Professor, Department of Civil Engineering, IIT Hyderabad, Kandi, Telangana 502284, India, Email: buma@ce.iith.ac.in, Tel +91 40 2301 6301, Fax +91 40-2301 6147.

ABSTRACT: The pullout resistance of reinforcement is an important parameter in the design of reinforced retaining structures. At incipient failure, the kinematics of failure in a reinforced retaining structure shows that the sliding mass of soil pulls the reinforcement obliquely along the slip surface. The response of reinforcement to oblique pull can be considered to be made up of equivalent axial and transverse components of the oblique pull. Accordingly, axial and transverse pullout tests were conducted on geostrip, and metal strip (both smooth and ribbed) reinforcements embedded in uniform sand. Ribbed metal strip reinforcement registered higher pullout resistance than smooth metal strip and geostrip reinforcements. The modified axial pullout resistance factors accounting for transverse pull ranged from 0.44 to 1.23, 1.4 to 3.5, and 2.0 to 5.2 for geostrip, smooth-metal-strip, and ribbed-metal-strip reinforcements, respectively. While the axial pullout resistance factors ranged from 0.34 to 0.65, 0.75 to 1.1, and 0.94 to 1.3.

Keywords

Reinforced soil; Geostrap; Metal strip; Axial pullout; Transverse pullout

1 Introduction and Background

The term *mechanically stabilized* is referred to as strengthening the soil by the inclusion of artificial reinforcement elements in the form of metal strips or geosynthetic elements. Inclusion of reinforcement improves the overall performance of the composite soil by restraining the tensile deformations of the soil through (a) interfacial bond resistance between soil and reinforcement, and (b) passive resistance against the transverse ribs.

In general, soil-reinforcement interaction is governed by two mechanisms - direct shear and pullout modes. In reinforced soil wall designs, pullout resistance of reinforcement is an important parameter to perform internal stability check. During this check, mobilization of tensile force in the reinforcement and its direction in the vicinity of the failure surface is considered. Localized mobilization of force in the reinforcement is dependent on the kinematics of failure of the reinforced structure. In general, the reinforcement intersects the slip surface transversely/obliquely (as shown in Figures. 1a & 1b, the portions 'E' and 'F') along the failure surface. The loci of maximum tension or the failure surface was linear at a failure angle of ($45+\varphi/2$) for extensible geostrip reinforcement and bilinear for inextensible metal strips as given in AASHTO, FHWA and other published literature (Elias, Christopher and Berg, 2001; Madhav and Umashankar, 2003b, 2003a; Shahu, 2007; Narasimha Reddy, Madhav and Saibaba Reddy, 2008a, 2009; Anderson *et al.*, 2010; Patra and Shahu, 2012; *AASHTO LFRD Bridge Design*. 9th edn, 2020) (Refer Figure 1).

The locus of maximum tension on the reinforcement at different layers clearly distinguishes the active and resistant zones and the minimum embedded or adherence length of the reinforcement in the retained zone is of interest in the internal stability check of the design. The minimum adherence length is in general based on the axial pullout resistance of the reinforcement (Khalid Farrag 1993; Ingold 1983; Fahmy et al. 1994; Sobhi and Wu 1996; Bergado et al. 2000; Abdelouhab et al. 2010; Palmeira 2009). The pullout load corresponding to a front-end displacement of 20 mm for inextensible reinforcements or a rear-end displacement of 15 mm for the extensible reinforcements is considered as the axial pullout resistance (Elias, Christopher and Berg, 2001).

However, many published literature studies (for example, Madhav and Umashankar 2003a; b; Narasimha Reddy et al. 2008a; b, 2009; Patra et al. 2015; Patra and Shahu 2012; Shahu 2007; Zornberg et al. 1998) suggest that the design for embedded or adherence length of the reinforcement in the resistant zone should consider the oblique pullout resistance considering the realistic kinematics of soil along the failure surface.

Zornberg et al. (1998) investigated the failure mechanisms of geosynthetic reinforced soil slopes using a centrifuge model. A slip mechanism passes through the toe of the embankment and corroborated the oblique pull of the geosynthetic reinforcement along the failure surface.

Analysis of an axial pull on a reinforcement is quite straight forward, where the normal stresses acting on the reinforcement-soil interface, q_t and q_b, being equal to gravity stresses (Fig. 2a). Therefore, the mobilized shear resistances at the interface (τ_t and τ_b) are proportional to normal stresses. When the reinforcement is subjected to transverse pull at one end (w_L), soil under the reinforcement mobilizes additional normal stresses (Δq_b) and thereby the mobilized shear resistance along the reinforcement increases (Fig. 2b). The increase in the pullout resistance improves the factor of safety against pullout.

Analytical models were firstly proposed by Madhav and Umashankar (2003a, 2003b) to predict the response of individual sheet reinforcement subjected to transverse pull or displacement. The proposed analytical models are valid for small transverse displacements of the order of 0.01 times the length of reinforcement, and hence the formulation is applicable only to small inclinations at the reinforcement end. (Madhav & Manoj 2004) extended the model to account for larger displacements and the inclinations of the reinforcement at the reinforcement end. In these models, the Winkler model was used to represent the soil and it has several limitations. Narasimha Reddy et al. (2008b, 2009) performed pseudo-static seismic analysis of reinforced soil wall considering oblique force or displacement using the horizontal slice method. Patra et al. (2015) and Patra and Shahu (2012) considered a two-layer Pasternak model to represent the soils to overcome the limitations observed in Winkler's model. Bhowmik et al. (2019) discussed the behavior of geogrid and geosynthetic sheet reinforcements under inclined pullout using large-scale inclined pullout apparatus. They concluded that the maximum pullout force increases by more than 20% as the inclination of pullout force increase from 0º to 30º in case of sheet and geogrid reinforcements.

Hariprasad and Umashankar (2018) discussed the behavior of smooth-metal-strip reinforcement embedded in sand bed and subjected to a transverse pull. However, the combined effect of axial and transverse pullout on the smooth metal strips was not reported. Karnamprabhakara et al. (2022; Karnamprabhakara and Balunaini (2021) reported the effect on accounitng the transverse pull on the reinforcement and proposed modified pullout resistance factors for polyester geogrids embedded in pond ash and waste foundry sand. There are certain studies on modelling the tensile loads and pullout loads of geostraps (Miyata, Bathurst and Allen, 2018, 2019). However, there are no pullout studies studies available on geostraps and metal strips considering the effect of transverse pull.

The present study is aimed at measuring the inherent additional pullout resistance of the geogrid at an assumed failure angle considering the actual or realistic oblique pullout force on the reinforcement. So, an extensive experimental program was carried out to study the response of geostrips and metal-strip (both smooth and ribbed) reinforcements subjected to axial and transverse pull. The effect of oblique pull was studied considering the equivalent transverse force as additional normal force on the reinforcement. The modified axial pullout resistance factors ($F^{*}_{axial|mod}$), duly considering the effect of transverse pull, were proposed at three different normal stresses.

2 Experimental Program

2.1 Materials used

Sand

Indian Standard (IS) Grade-II sand, widely known under the name of Ennore sand, IS 650:1991 was used. Table 1 provides the properties of the dry Ennore sand used in the study from testing, and it was classified as poorly graded sand (SP) as per USCS classification. The shape of sand particles was found to be sub-angular to angular. More details of the Ennore sand can be found in Hariprasad et al. (2016).

Reinforcement

Reinforcements in soil were broadly categorized into inextensible and extensible. Reinforcements that deform less than the surrounding soil are classified as *inextensible reinforcements* (e.g., metal strips, metal grids), while reinforcement that deforms as much as surrounding soil are classified as *extensible reinforcements* (e.g., geostrips, geogrids). In the present study, an extensible reinforcement (geostrip) and inextensible reinforcements (metal strips) were used to study the axial and transverse pullout responses.

i. Geostrip

The geostrip reinforcement used in this study consisted of discrete channels of closely packed, high-tenacity polyester fibers encased in a polyethylene sheath. The width and thickness of geostrip were equal to 90 mm and 3 mm, respectively. The tensile strength of the geostrip was equal to about 100 kN.

ii. Metal strips

The top and bottom surfaces of the ribbed metal strip had pairs of 3 mm-high ribs, equally spaced at 110 mm along its length. The configuration of smooth-metal-strip was same as that of ribbed-metal strip, but surface of the reinforcement was filed to remove the ribs from the surface of the strip. The width and thickness of metal strips were equal to 40 mm and 4 mm, respectively. More details on the metal strips can be found in Hariprasad and Umashankar (2018).

2.2 Pullout test apparatus

A unique test frame which facilitates to conduct pullout testing on various reinforcements in axial and transverse directions, individually, was used in the present study. The major components of the test frame include axial pullout setup, transverse pullout setup, test sample box, normal load application unit, power control panel, and hydraulic control unit. The schematic view of the unique pullout test frame, highlighting the important components of the system can be found in Karnamprabhakara et al. (2021). Stationary pluviation device with adjustable heights was used to prepare uniform sand beds. Needle flow valves installed in the axial and transverse pullout flow lines, will aid in using one pullout setup at a time.

The size of the sample test box used in this study was equal to 900 mm (in length), 900 mm (in width), and 1000 mm (in depth). The normal loading unit comprises of a rigid plate of dimensions 890 mm x 890 mm (in plan), connected to a hydraulic cylinder and guide rods for uniform movement of the plate during testing. The power control panel and hydraulic control unit were used in parallel for pumping the oil into the various cylinders in the circuit, and also for their upward and downward movements. Detailed description of Pluviation device can be found in Hariprasad et al. (2016), axial pullout test setup and its components in Karnamprabhakara et al. (2021), and more details on the transverse pullout test setup in Hariprasad and Umashankar (2018).

Test procedure

Smooth polythene sheets were glued to the inner walls of test chamber to reduce the friction along the walls during the application of normal stress. During the Pluviation process, the height of fall and sieve opening width to pluviate the sand particles were maintained as 150 mm and 2 mm. Average relative density of sand bed of about 85% was achieved during sample preparation. Throughout the testing, uniform sand beds were ensured from the Pluviation method. The spatial variability in the sample preparation was discussed in Hariprasad et al. (2016). The effective length (L_e) of the reinforcements used in the axial and transverse pullout testing was equal to 850 mm. The reinforcements were placed at mid heights underlying the prepared sand beds and were firmly clamped in the U-groove of the clamping system with the help of bolt and screw arrangement. To hold the reinforcements within the U-groove, they were sandwiched between two thin mild steel tabs to avoid slippage during axial and transverse pullout tests. A sleeve of 32 mm was used in the axial pullout system to avoid the passive resistance developed at the front-face of the chamber. The clamping levels for axial and transverse pullout are at 520 mm, and 400 mm from the bottom of the test chamber. However, rigid concrete blocks of depth 200 mm were placed at the bottom of the test chamber during axial pullout testing, considering the effort in preparing the sample. The effective depth of the sample for axial pullout testing was equal to 640 mm with reinforcement placed at mid-height.

Both the axial and transverse pullout tests on the three reinforcements considered were tested under three normal stresses equal to 17 kPa, 52 kPa, and 87 kPa. The unit weight (γ) of the pluviated sand was equal to 17.1 kN/m^3, and the depth, D_e, of reinforcement was equal to 320 mm and 400 mm, for axial and transverse pullout samples, respectively. In case of axial pullout testing, the reinforcement was pulled axially at a constant pullout rate of 1 mm/minute, whereas, in case of transverse pullout testing, transverse pullout load was applied on the reinforcement in incremental mode for a given normal stress in accordance with (ASTM D6706, 2006). The pullout resistance during the axial and transverse pull of the reinforcements were recorded using the axial and transverse pullout load cells, respectively. The axial and transverse pullout displacements of the reinforcement were taken as the average of the readings measured from the two potentiometers. More details of the equipment, working mechanism, and data recording are available in Karnamprabhakara et al. 2021; Hariprasad and Umashankar 2018.

3 Results and Discussion

The axial and transverse pullout responses of geostrip, smooth and ribbed metal strip reinforcements embedded in uniformly prepared sand beds were discussed in the following sections. The response of reinforcement to oblique pull for a given normal stress on the reinforcement was accounted by considering the transverse pullout as an additional normal stress on the reinforcement to the applied normal stress. Accordingly, the axial pullout resistance factors and the modified axial pullout resistance factors were presented in the following sections.

3.1 Pullout resistance of geostrip

Figures 3a and 3b show the axial and transverse pullout response of geostrip reinforcement under the normal stresses of 17 kPa, 52 kPa, and 87 kPa. The pullout force was observed to increase with the front-end axial pullout displacement and reaches a limiting value in the range of 5 mm-10 mm displacement (Fig. 4a). An expected increase in the axial pullout force with an increase of normal stress was also observed. The pullout response of geostrip reinforcement mainly depends on frictional resistance mobilized between the soil and the surface of reinforcement. In the case of transverse pullout, at a given normal stress, no limiting value of pullout force was attained, and the transverse pullout force was found to increase continuously with the transverse displacement for the range of displacement (=30 mm) considered in this study (Fig. 4b). This behavior could be attributed to the increase in normal stress from the soil elements underneath the strip due to transverse pull of the reinforcement at its one end, leading to an increase in the mobilized shear resistance between soil and reinforcement (as shown in Fig. 2). For instance, it could be observed that the transverse pullout force increased by 38%, when the transverse displacement of the reinforcement increases from 15 mm to 20 mm under normal stress of 87 kPa.

3.2 Pullout resistance of metal strips

The axial and transverse pullout behavior of smooth-metal-strip reinforcement under three normal stresses were presented in Figures (4a and 4b). The axial pullout resistance increased with the increase in normal stress on the reinforcement. In case of axial pullout testing, the smooth metal strips reached a limiting pullout force in the range of axial pullout displacement of 5 mm-10 mm (Fig. 5a), and the load was nearly constant after reaching the limiting pullout force. At this stage, the limiting interface shear stress along the entire length of the metal strip reinforcement has been attained. In the case of transverse pullout testing, the pullout force was found to increase continuously with the displacement due to the mobilization of additional normal stresses on the reinforcement due to transverse pull (Hariprasad and Umashankar 2018).

Figures 5a and 5b show the pullout response of a ribbed-metal-strip reinforcement subjected to axial and transverse pull. The pullout force in the case of ribbed metal strips is due to the frictional resistance mobilized between the surface of reinforcement and sand and the passive resistance against the transverse ribs. High axial and transverse pullout forces for ribbed-metal-strip reinforcement can be attributed to the additional passive resistance from the transverse ribs in comparison with the smooth metal strips. According to studies reported in the literature (Huang, Bathurst and Allen, 2012; Miyata and Bathurst, 2012), axial pullout resistance of reinforcement was higher in the case of ribbed-metal-strip reinforcement compared to smooth-metal-strip reinforcement. In the case of ribbed-metal-strip, the limiting pullout resistance during axial pull was observed at a front-end displacement in the range of 15 mm-20 mm (Fig. 6a). In the case of transverse pullout testing performed at a given normal stress, no limiting value of pullout force was attained, and the transverse pullout force was found to increase continuously with displacement for the range of displacements considered in this study (Fig. 6b). The behavior was similar to that of smooth metal strips. For instance, ribbed-metal-strip tested under a normal stress equal to 87 kPa, the transverse pullout force was found to increase by 58% when the transverse displacement of the reinforcement increases from 15 mm to 20 mm.

For all the normal stresses considered in the study, higher transverse pullout force was noticed in the case of ribbed-metal-strip reinforcement compared to smooth-metal-strip reinforcement at a given displacement. For instance, transverse pullout force for ribbed-metal-strip was higher than that of smooth-metal-strip reinforcement by 36%, 17%, and 27% corresponding to a transverse displacement of 20 mm corresponding to normal stresses of 17 kPa, 52 kPa, and 87 kPa, respectively. This increase in transverse pullout force can be attributed to the additional passive resistance coming from the transverse ribs in the ribbed metal strip.

3.3 Pullout resistance factor (F^*)

In the design of mechanically stabilized structures, the pullout resistance factor, F^*, between the reinforcement and the backfill material is used to estimate the pullout resistance of reinforcement (Eq. 1) (Elias et al. 2001).

$$P_{ult} = F^{*}.\ \alpha.\ L_e.\ b.\ C.\ \sigma_n \quad (1)$$

where, P_{ult} is the ultimate pullout resistance of the reinforcement, α is the correction factor to account for the non-linear shear stress distribution along the reinforcement (in general, taken as 0.6-1 for geosynthetic reinforcements and 1 for metallic reinforcements), σ_n is the normal stress acting on the reinforcement, L_e is the embedment length of the reinforcement in the resisting zone, b is the width of the reinforcement, and C is the effective unit perimeter (= 2, in general).

The variation of F^* values of reinforcements with the equivalent depth, Z_{eq}, of reinforced wall (that correspond to various normal stresses) were plotted for both the axial and transverse pullout testing.

Figure 6a shows the typical failure surface of the reinforced soil structure with extensible reinforcement of height, H, with an angle of inclination, θ_f, to the horizontal. The failure surface intersects the reinforcement obliquely and the oblique pullout of reinforcement was shown as $P_{i, oblique}$, and the corresponding oblique pullout displacement that reinforcement undergoes along the failure surface was shown as δ. The corresponding axial and transverse components are $\delta\cos\theta_f$ and $\delta\sin\theta_f$, respectively (refer to Fig. 7b). In other words, the oblique pullout, $P_{i, oblique}$, can be resolved into components along axial and transverse directions of the reinforcements and were equal to $P_{r, axial}$, and $P_{r, trans}$, respectively. The transverse pullout force ($P_{r, trans}$) on the reinforcement will impose additional vertical force on the reinforcement, thus leading to enhanced pullout resistance of reinforcement along the axial direction. It should be noted that reinforced soil structure with inextensible reinforcements will have a bilinear failure as shown in Figure 1b, and the upper half of the wall will be subjected to transverse pullout alone.

The pullout resistance factors were proposed for all the reinforcements embedded in uniform sand beds under three normal stresses. To define pullout resistance factors, the Federal Highway Authority (FHWA) suggests considering the axial pullout resistance at a rear end displacement of 15 mm, and 20 mm for extensible and inextensible reinforcements, respectively. However, the present study emphasizes the effect of oblique pullout of reinforcement. Thereby, the pullout resistance factors were defined for an assumed oblique pullout displacement (=δ) of 30 mm. The corresponding axial (=$\delta\cos\theta_f$) and transverse (=$\delta\sin\theta_f$) pullout displacements were equal to 12 mm (or the displacement corresponding to peak pullout resistance) and 27 mm, respectively, considering the angle of shearing resistance of sand particles equal to 42° (Hariprasad and Umashankar 2018).

Thus, the axial and transverse pullout resistance factors were defined at the resolved displacements using the Equations 2 and 3.

Axial pullout resistance factor, $$F^*_{axial} = \frac{P_{r,axial}}{\alpha.L_e.b.C.\sigma_n} \quad (2)$$

Transverse pullout resistance factor, $$F^*_{trans} = \frac{P_{r,trans}}{\alpha.L_e.b.C.\sigma_n} \quad (3)$$

where α was considered equal to 1 for both geostrip and metallic strip reinforcements, and C was equal to 2.

The transverse pullout force was considered as the additional force on the reinforcement and the modified or improved axial pullout resistance, $P_{r,\ axial|mod}$, was calculated using the following equation 5,

$$P_{r,axial|\mathrm{mod}} = [\sigma_n.\alpha.L_e.b.C + P_{r,trans}].F^*_{axial} \quad (4)$$

Using equation 3 in equation 4, the modified axial pullout resistance is equal,

$$P_{r,axial|\mathrm{mod}} = [F^*_{axial}.\sigma_n.\alpha.L_e.b.C + F^*_{trans}.\sigma_n.\alpha.L_e.b.C.F^*_{axial}] \quad (5)$$

From the definition of ultimate pullout resistance of reinforcement from FHWA, the modified axial pullout resistance factor is defined as in Equation 6,

$$F^*_{axial|\mathrm{mod}} = \frac{P_{r,axial|\mathrm{mod}}}{\alpha.L_e.b.C.\sigma_n} \quad (6)$$

Equating equations 5 and 6,

$$F^*_{axial|\mathrm{mod}} = F^*_{axial}(1 + F^*_{trans}) \quad (7)$$

Figures (7a, 7b, and 7c) show the axial, transverse, and modified pullout resistance factors for the reinforcements (geostrip, smooth-metal-strip, and ribbed-metal-strip reinforcements) plotted against equivalent depth as well as the normal stresses at that level of the reinforcement. Pullout resistance factors for ribbed-metal-strip reinforcements were higher compared to smooth-metal-strip reinforcements for all the cases due to mobilization of passive resistance against the ribs on the surface of reinforcement.

The variation of the pullout resistance factors due to axial and transverse pull with the equivalent depth of the reinforced wall showed similar trends for all the reinforcements tested. The pullout resistance factors were found to decrease with an increase in the equivalent depth. The higher pullout resistance factors at lower depths were due to dilation occurring near the surface of the reinforcement (Hariprasad and Umashankar 2018). The modified axial pullout factors ($F^*_{axial|mod}$) were much higher in comparison with the axial and transverse pullout factors, because of the consideration of the effect of the transverse pull on the axial pullout resistance due to the mobilization of additional normal stresses under transverse pull. The modified axial pullout factors ($F^*_{axial|mod}$) were found to be in the range of 0.44 - 1.23, 1.4 - 3.5, and 2 - 5.2 for geostrip, smooth-metal-strip, and ribbed-metal-strip reinforcements, respectively. While, F^*_{axial} values considering only axial pull were found to range from 0.34 - 0.65, 0.75 - 1.1, and 0.94 - 1.3, respectively.

In case of inextensible reinforcements considered in the present study, the proposed transverse pullout resistance factors can be used in the design of reinforced soil wall for the upper half height of the wall, and the modified axial pullout resistance factors can be used for the lower half of the wall.

It could be noted that the entire analysis in the present study was carried out for a limit state equilibrium using tie-back wedge analysis and coherent gravity methods for extensible and inextensible reinforcements. However, the present analysis could be extended with the stiffness method proposed by AASHTO (2020).

4 Conclusions

A unique large-scale pullout apparatus capable of performing axial pull and transverse pull of the reinforcements was used to study the axial and transverse pullout responses of extensible (geostrip) and inextensible (smooth-metal strip and ribbed-metal strip) reinforcements. The major findings from the study are as follows:

a) For three different normal stresses used in the study, the limiting axial pullout force was observed at a front-end displacement ranging between 5 -10 mm for both the extensible and inextensible reinforcements. Whereas the transverse pullout force was found to increase continuously with the pullout displacement due to the mobilization of additional normal stresses in the soil elements underneath the reinforcement during the downward pull.

b) The axial and transverse pullout forces of ribbed-metal-strip was found to be high in comparison with smooth-metal-strip. The axial (F_{axial}^*) pullout resistance factors of geostrip, smooth-metal-strip, and ribbed-metal-strip reinforcement ranged from 0.34 to 0.65, 0.7 to 1.08, and 0.93 to 1.27, respectively. Similarly, the transverse pullout resistance factors (F_t^*) ranged from 0.29 to 0.88, 0.9 to 2.1, and 1.2 to 3.0, respectively.

c) The modified axial pullout resistance factor ($F^*_{axial|mod}$) considering the effect of transverse pull on the reinforcement were found to be higher than the conventional axial pullout resistance factor (F^*_{axial}) for all the reinforcements considered. The modified axial

($F_{axial|mod}^{*}$) pullout resistance factors for geostrip, smooth-metal-strip, and ribbed-metal-strip reinforcements ranged from 0.44 to 1.23, 1.4 to 3.5, and 2.07 to 5.2, respectively.

The proposed modified axial pullout resistance factors ($F^{*}_{axial|mod}$) may be helpful to perform a realistic design of MSEW and RSS structures.

List of notations

F^{*} - Pullout resistance factor (dimensionless)

F^{*}_{axial} - Axial pullout resistance factor (dimensionless)

F^{*}_{trans} - Transverse pullout resistance factor (dimensionless)

$F^{*}_{axial|\mathrm{mod}}$ - Modified axial pullout resistance factor (dimensionless)

C - Reinforcement effective unit perimeter (dimensionless)

b - Width of the reinforcement (m)

L_e - Effective length of the reinforcement (m)

σ_n - Normal stress on the reinforcement (Pa)

α - Correction factor for non-linear stress distribution over embedded length (dimensionless)

$P_{r,axial}$ - Axial pullout force (kN)

$P_{r,trans}$ - Transverse pullout force (kN)

P_{ult} - Ultimate pullout resistance force (kN)

γ - Unit weight of the sand (kN/m^3)

φ - Angle of shearing resistance (in degrees)

q_t - Normal stress on the top of the reinforcement (kPa)

q_b - Normal stress on the bottom of the reinforcement (kPa)

τ_t -Mobilized shear resistance on the top of the reinforcement at the interface (kPa)

τ_b - Mobilized shear resistance on the bottom of the reinforcement at the interface (kPa)

Δq_b - Additional normal stress on the reinforcement (kPa)

D_e - Effective depth of the reinforcement from the top in the test box (m)

Z_{eq} - Equivalent depth of the reinforcement (m)

θ_f - Failure angle (in degrees)

δ - Oblique pullout displacement (mm)

List of Abbreviations

ASTM- American Standard of Testing Materials

FHWA- Federal Highway Authority

IS- Indian Standard

MSE- Mechanically Stabilized Earth

USCS- Unified Soil Classification System

Data Availability Statement

All data, models, and code generated or used during the study appear in the submitted article.

Acknowledgments

Authors thank the Reinforced Earth India Pvt. Ltd, India; and Maccaferri Environmental Sol. Pvt. Ltd, for their support in providing the metal strips and geostrip samples, respectively, used in this study. The contents of this paper reflect the views of the authors, who are solely responsible for the facts and accuracy of the data presented herein.

References

AASHTO LFRD Bridge Design. 9th edn (2020). Washington, DC.

Abdelouhab, A., Dias, D. and Freitag, N. (2010) ‘Physical and analytical modelling of geosynthetic strip pull-out behaviour’, *Geotextiles and Geomembranes*, 28(1), pp. 44–53. Available at: https://doi.org/10.1016/j.geotexmem.2009.09.018.

Anderson, P.L. *et al.* (2010) *Coherent Gravity: The Correct Design Method for Steel-Reinforced MSE Walls*.

ASTM D6706 (2006) ‘Standard Test Method for Measuring Geosynthetic Pullout Resistance in Soil 1’.

Bergado, D.T., Teerawattanasuk, C. and Long, P. V (2000) ‘Localized mobilization of reinforcement force and its direction at the vicinity of failure surface’, *Geotextiles and Geomembranes*, 18, pp. 311–331.

Bhowmik, R., Shahu, J.T. and Datta, M. (2019) ‘Experimental studies on inclined pullout behaviour of geosynthetic sheet Vis-À-Vis geogrid - Effect of type of anchor and sand’, *Geotextiles and Geomembranes*, 47(6), pp. 767–779. Available at: https://doi.org/10.1016/j.geotexmem.2019.103490.

Elias, V., Christopher, B. and Berg, Ryan.R. (2001) ‘Mechanically stabilized earth walls and reinforced soil slopes design & construction guidelines’, *FHWA-NHI-00-043 Report* [Preprint].

Fahmy, R.F.W., Koerner, R.M. and Sansone, L.J. (1994) ‘Experimental behavior of polymeric geogrids in pullout’, *Journal of Geotechnical Engineering*, 120(4), pp. 661–677.

Hariprasad, C., Rajashekhar, M. and Umashankar, B. (2016) ‘Preparation of uniform sand specimens using stationary pluviation and vibratory methods’, *Geotechnical and Geological Engineering*, 34(6), pp. 1909–1922. Available at: https://doi.org/10.1007/s10706-016-0064-0.

Hariprasad, C. and Umashankar, B. (2018) ‘Transverse pullout response of smooth-metal-strip reinforcements embedded in sand’, *Journal of Geotechnical and Geoenvironmental Engineering*, 144(3), p. 06017020. Available at: https://doi.org/10.1061/(ASCE)GT.1943-5606.0001838.

Huang, B., Bathurst, R.J. and Allen, T.M. (2012) ‘LRFD Calibration for Steel Strip Reinforced Soil Walls’, *Journal of Geotechnical and Geoenvironmental Engineering*, 138(8), pp. 922–933. Available at: https://doi.org/10.1061/(ASCE)GT.1943-5606.0000665.

Ingold, T.S. (1983) ‘Laboratory Pull-Out Testing of Grid Reinforcements in Sand’, *Geotechnical Testing Journal*, 6(3), pp. 101–111.

Karnamprabhakara, B.K. *et al.* (2022) ‘Evaluation of interaction properties of uniaxial geogrids with waste foundry sand’, *Geosynthetics International* [Preprint]. Available at: https://doi.org/10.1680/jgein.21.00005a.

Karnamprabhakara, B.K. and Balunaini, U. (2021) ‘Modified axial pullout resistance factors of geogrids embedded in pond ash’, *Geotextiles and Geomembranes*, 49(5), pp. 1245–1255. Available at: https://doi.org/10.1016/j.geotexmem.2021.04.003.

Karnamprabhakara, B.K., Balunaini, U. and Arulrajah, A. (2021) ‘Development of a Unique Test Apparatus to Conduct Axial and Transverse Pullout Testing on Geogrid Reinforcements’, *Journal of Materials in Civil Engineering*, 33(1), pp. 1–11. Available at: https://doi.org/10.1061/(ASCE)MT.1943-5533.0003497.

Khalid Farrag, Y.B.A. and I.J. (1993) ‘Pull-Out Resistance of Geogrid Reinforcements’, *Geotextiles and Geomembranes*, 12, pp. 133–159.

Madhav, M.R. and Manoj, T.P. (2004) ‘Reinforcement – Soil Interactions under Transverse and Oblique Forces’, *12th ARC*, 2(1).

Madhav, M.R. and Umashankar, B. (2003a) ‘Analysis of inextensible sheet reinforcement subject to downward displacement / force : non- linear subgrade response’, (3), pp. 69–84.

Madhav, M.R. and Umashankar, B. (2003b) ‘Analysis of inextensible sheet reinforcement subject to transverse displacement / force : linear subgrade response’, 21, pp. 69–84. Available at: https://doi.org/10.1016/S0266-1144(03)00002-5.

Miyata, Y. and Bathurst, R.J. (2012) ‘Analysis and calibration of default steel strip pullout models used in Japan’, *Soils and Foundations*, 52(3), pp. 481–497. Available at: https://doi.org/10.1016/j.sandf.2012.05.007.

Miyata, Y., Bathurst, R.J. and Allen, T.M. (2018) ‘Evaluation of tensile load model accuracy for PET strap MSE walls’, *Geosynthetics International*, 25(6), pp. 656–671. Available at: https://doi.org/10.1680/jgein.18.00032.

Miyata, Y., Bathurst, R.J. and Allen, T.M. (2019) ‘Calibration of PET strap pullout models using a statistical approach’, *Geosynthetics International*, 26(4), pp. 413–427. Available at: https://doi.org/10.1680/jgein.19.00026.

Narasimha Reddy, G. v., Madhav, M.R. and Saibaba Reddy, E. (2008a) ‘Analysis of reinforced soil wall based on kinematics - Effect of transverse displacement’, *International Journal of Geotechnical Engineering*, 2(2), pp. 143–151. Available at: https://doi.org/10.3328/IJGE.2008.02.02.143-151.

Narasimha Reddy, G. v., Madhav, M.R. and Saibaba Reddy, E. (2008b) ‘Pseudo-static seismic analysis of reinforced soil wall-Effect of oblique displacement’, *Geotextiles and*

Geomembranes, 26(5), pp. 393–403. Available at: https://doi.org/10.1016/j.geotexmem.2008.02.002.

Narasimha Reddy, G. v., Madhav, M.R. and Saibaba Reddy, E. (2009) 'Kinematics and analysis of reinforced soil wall-linear backfill response', *International Journal of Geotechnical Engineering*, 3(1), pp. 39–50. Available at: https://doi.org/10.3328/IJGE.2009.03.01.39-50.

Palmeira, E.M. (2009) 'Soil–geosynthetic interaction: Modelling and analysis', *Geotextiles and Geomembranes*, 27(5), pp. 368–390. Available at: https://doi.org/10.1016/j.geotexmem.2009.03.003.

Patra, S. and Shahu, J.T. (2012) 'Pasternak model for oblique pullout of inextensible reinforcement', *Journal of Geotechnical and Geoenvironmental Engineering*, 138(12), pp. 1503–1513. Available at: https://doi.org/10.1061/(ASCE)GT.1943-5606.0000720.

Patra, S., Shahu, J.T. and Geosynthetics, I. (2015) 'Behaviour of extensible reinforcement resting on non-linear Pasternak subgrade subjected to oblique pull', 2(9), pp. 770–779.

Shahu, J.T. (2007) 'Pullout response of inextensible sheet reinforcement subject to oblique end force', *Journal of Geotechnical and Geoenvironmental Engineering*, 133(11), pp. 1440–1448. Available at: https://doi.org/10.1061/(ASCE)1090-0241(2007)133:11(1440).

Sobhi and Wu (1996) 'An interface pullout formula for extensible sheet reinforcement', *Geosynthetics International*, 3(5), pp. 565–582.

Zornberg, J.G., Sitar, N. and Mitchell, J.K. (1998) 'Performance of geosynthetic reinforced slopes at failure', *Journal of Geotechnical and Geoenvironmental Engineering*, 124(8), pp. 670–683. Available at: https://doi.org/10.1061/(ASCE)1090-0241(2000)126:3(281).

Figures

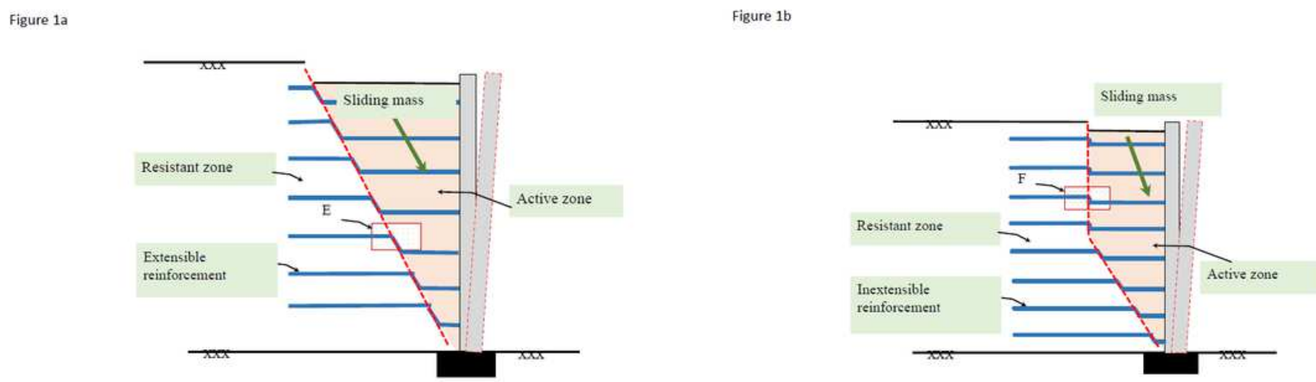

Figure 1

Mechanism at limit state for reinforced soil structures with, (a) extensible reinforcement, and (b) inextensible reinforcement

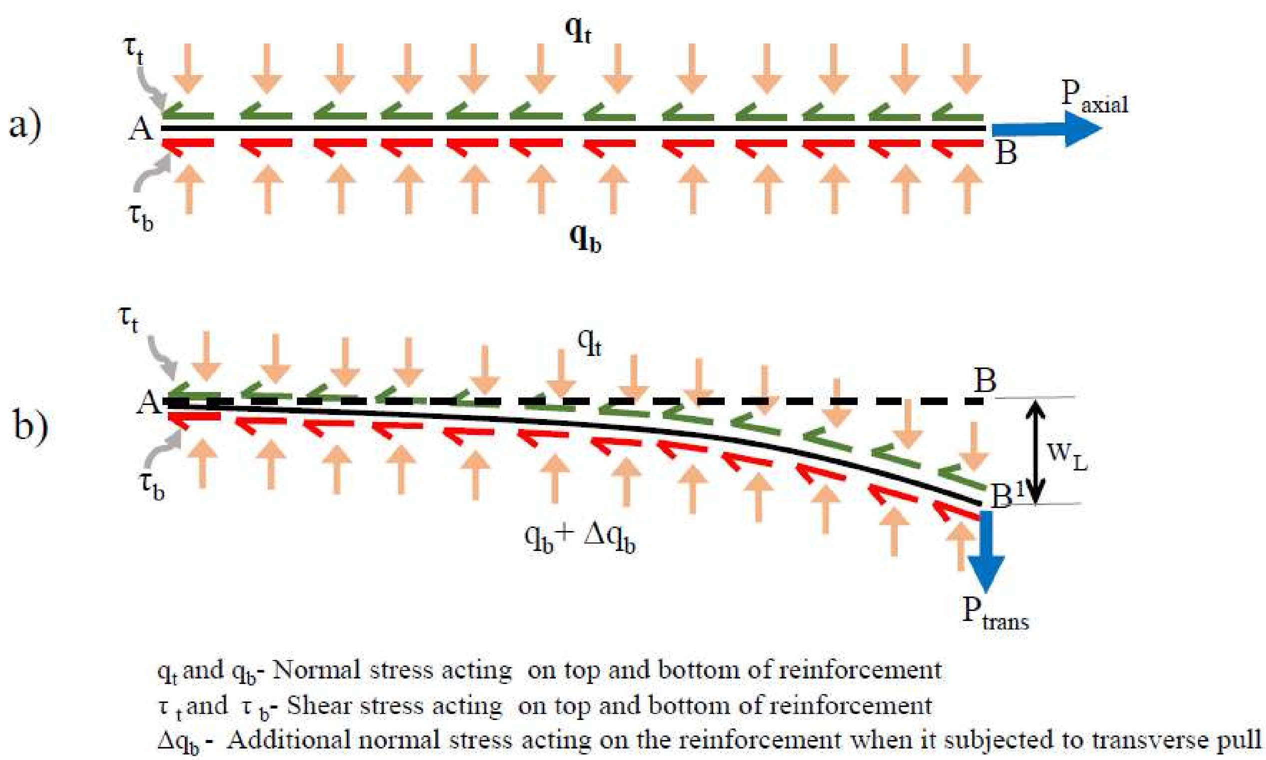

Figure 2

Pullout mechanism: reinforcement subjected to (a) axial pull, and (b) transverse pull

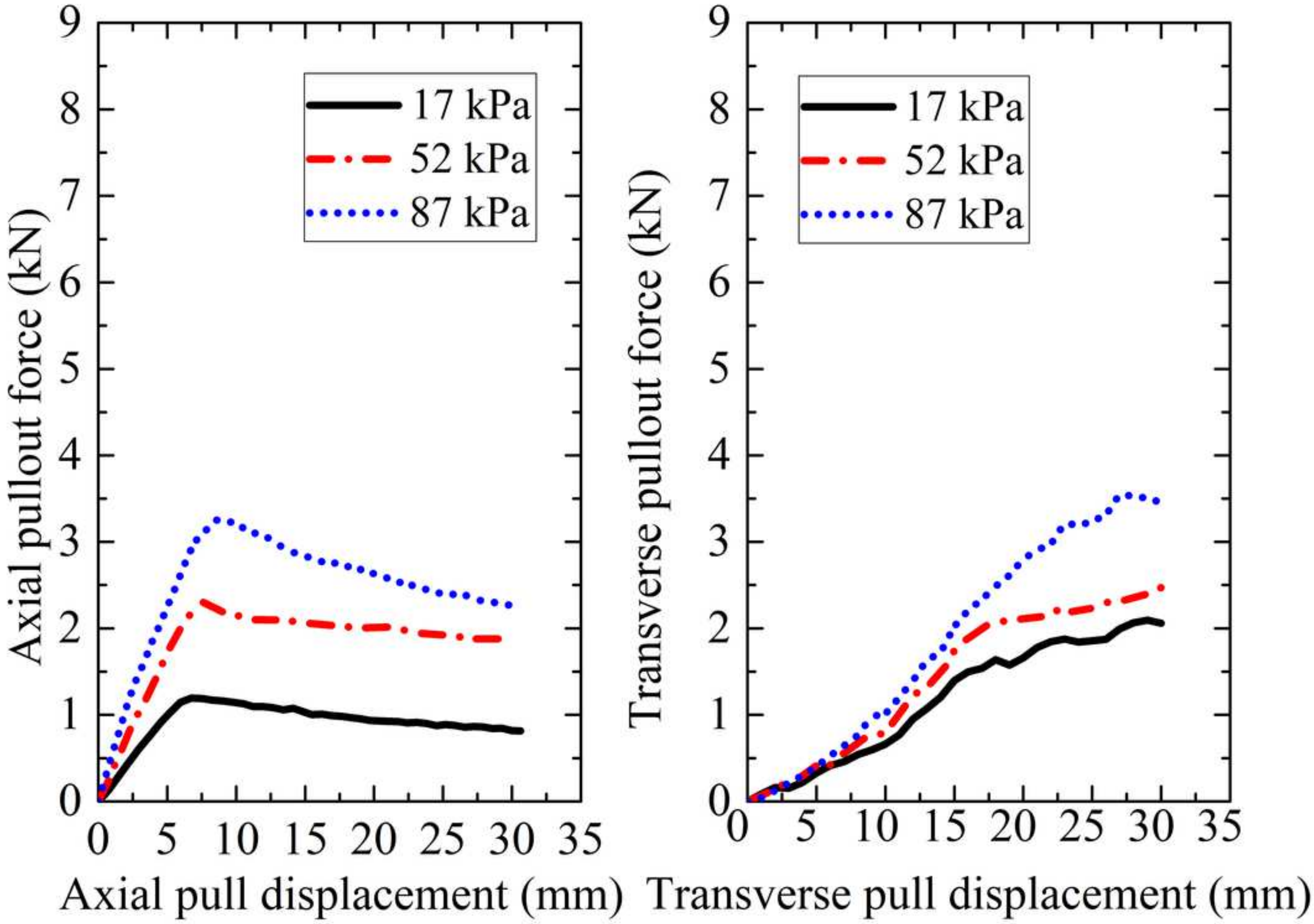

Figure 3

Pullout behaviour of geostrip reinforcement: (a) axial pullout, and (b) transverse pullout

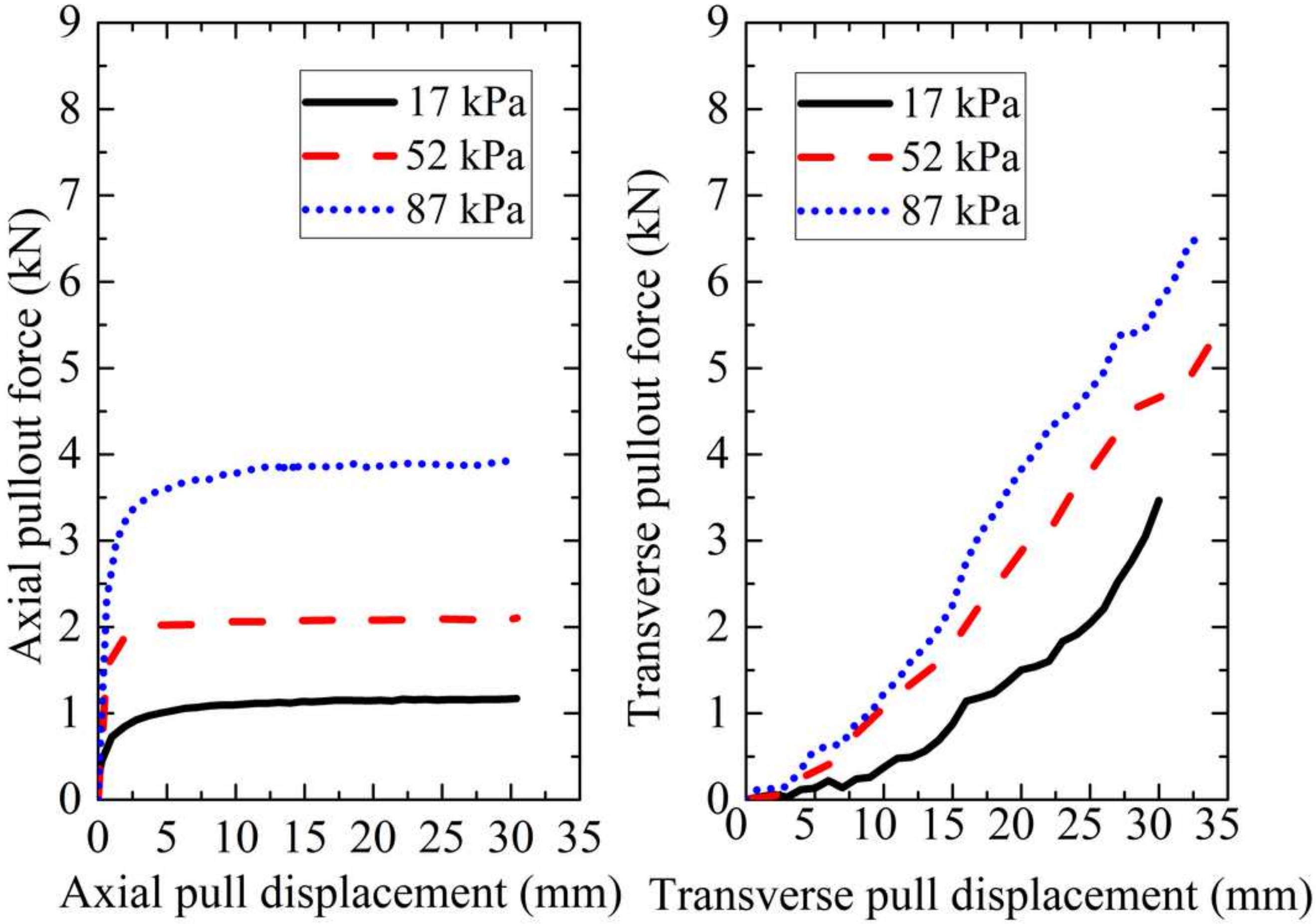

Figure 4

Pullout behaviour of smooth-metal-strip reinforcement: (a) axial pullout, and (b) transverse pullout (Hariprasad and Umashankar, 2018)

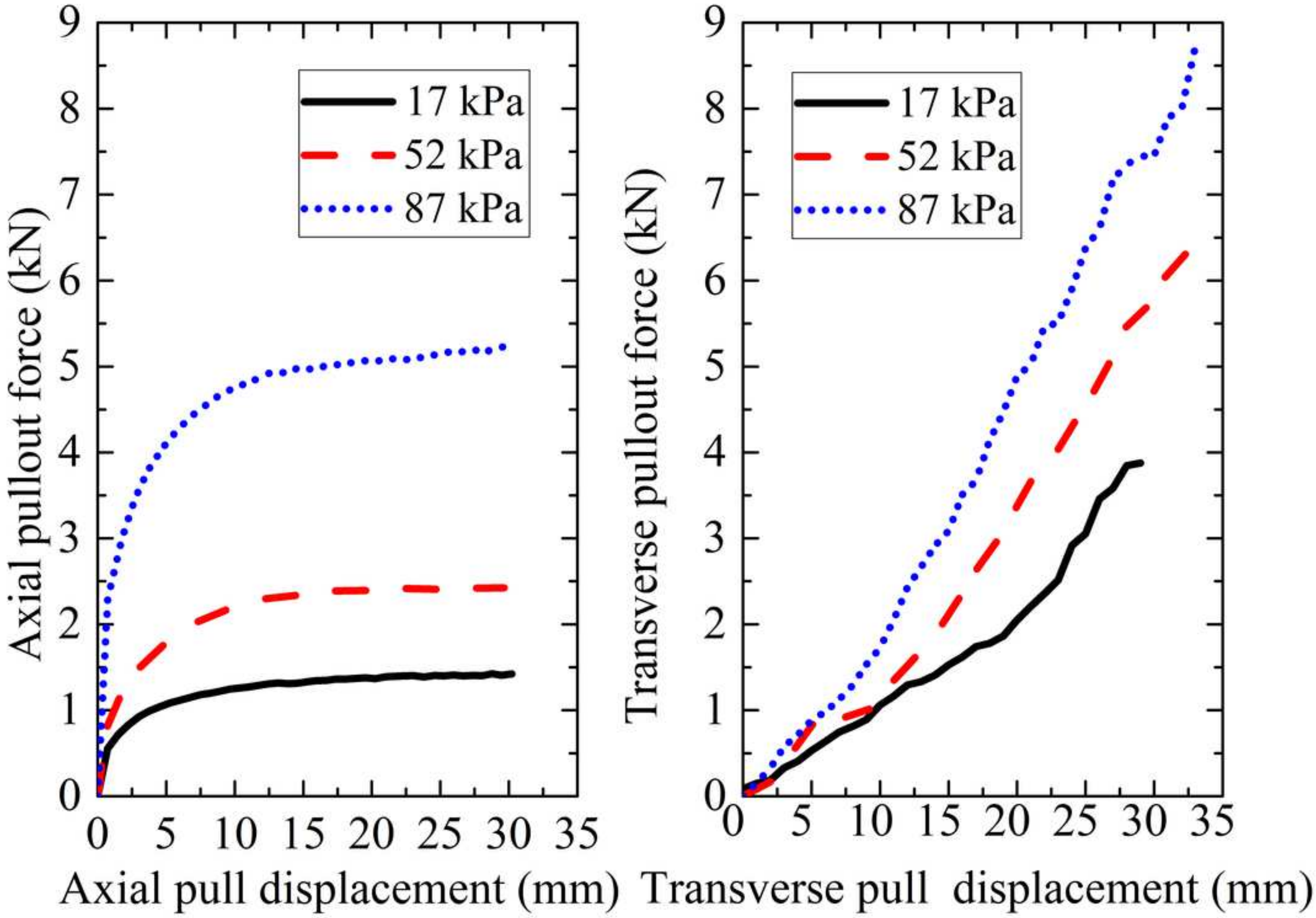

Figure 5

Pullout behaviour of ribbed-metal-strip reinforcement: (a) axial pullout, and (b) transverse pullout

Figure 6A

Figure 6B

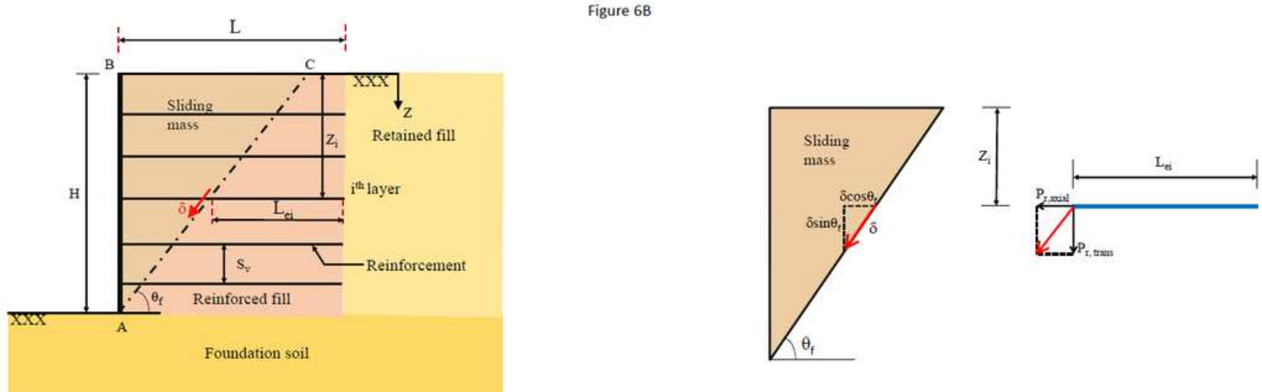

Figure 6

Oblique pull/displacement: (a) at a depth z_i from the surface of the reinforced wall, and (b) representation of forces along the reinforcement

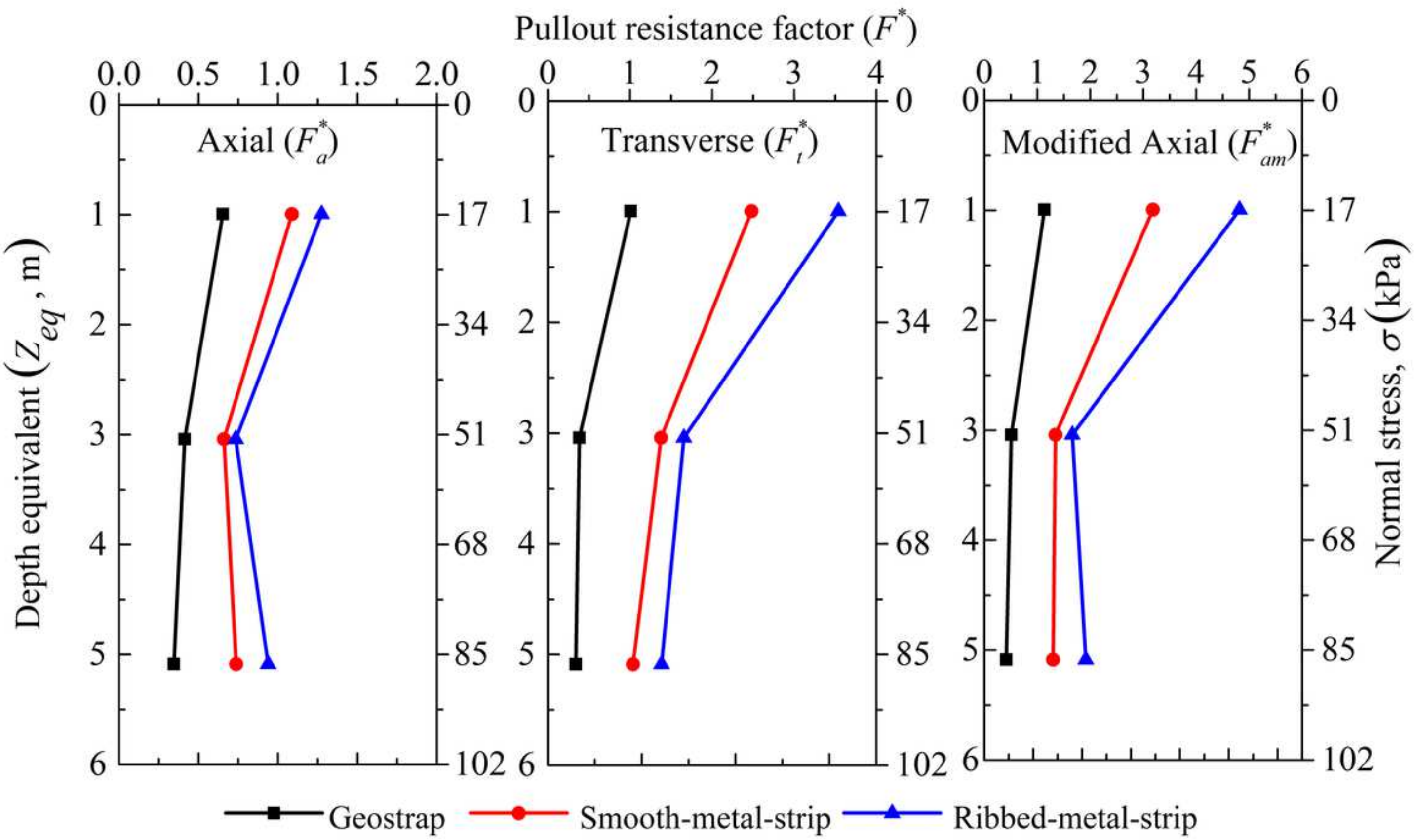

Figure 7

Pullout resistance factors considering: (a) axial pullout, (b) transverse pullout, and (c) modified axial pullout

Supplementary Files

This is a list of supplementary files associated with this preprint. Click to download.

- ListofTables.docx